Modeling Airside Congestion Dynamics Using Macroscopic Fundamental Diagram: Insights and Applications

Hasnain Ali, Xuan Tao Hoo, Thai Van Phat, Duc-Thinh Pham, Sameer Alam
Air Traffic Management Research Institute,
School of Mechanical and Aerospace Engineering,
Nanyang Technological University, 637460, SINGAPORE

***Abstract*—Airport airside congestion, driven by the growing imbalance between air traffic demand and constrained capacity, presents significant operational challenges. To address this, there is a critical need for effective models that capture the complex interactions within the airside (taxiway-runway-gate) system and provide insights into traffic flow dynamics and congestion mechanisms. Traditional approaches, such as microsimulation and queuing models, although detailed, tend to focus on individual components without capturing the broader interactions within sub-systems. This limitation, combined with high computational demands, restricts their effectiveness for real-time applications. This study proposes adapting the Macroscopic Fundamental Diagram (MFD) to model airside traffic using three-dimensional aircraft trajectory data. By focusing on aggregate traffic variables—flow, density, and speed—the MFD offers a computationally efficient approach to understanding airside congestion patterns and informed decision-making.**

This paper presents a novel methodology for constructing airside MFDs using A-SMGCS data from Singapore Changi Airport. The study also investigates the spatial and temporal factors contributing to congestion, offering insights into how congestion patterns develop and evolve under varying operational conditions. In the temporal domain, even during low-demand periods, departure and arrival banks contribute to congestion. In the spatial domain, traffic inhomogeneity—an uneven distribution of traffic on the airside network—reduces overall flow, particularly during congestion. These findings highlight the potential to improve airside capacity utilization and mitigate congestion by distributing traffic more evenly across both temporal and spatial domains, i.e., minimizing schedule banks and ensuring a balanced allocation of taxi routes.

***Keywords*—Macroscopic Fundamental Diagram; Airside Congestion; Demand Banking; Inhomogenous Taxi-routes.**

I. Introduction

Airport airside is a complex system, characterised by non-linear and non-hierarchical interactions between humans (air traffic controllers (ATCOs), pilots), machines (aircraft, navigation aids), procedures (safe separation, pushback procedures, delay management), and environment (runway, taxiway, gate etc.). Globally, the growing disparity between increasing air traffic demand and constrained airside capacity is leading to congestion [1]. To mitigate airside congestion, it is critical to understand the interactions between traffic demand and airside capacity, along with developing effective models that capture traffic flow characteristics and the mechanisms by which congestion forms, spreads, and dissipates. Existing airside modeling approaches either focus on detailed aircraft trajectories [2] or specific subsystems (like runways) [3], failing to capture the full complexity of interactions across the entire airside network. In this context, there is a need for airside traffic models that can robustly describe the interactions among various stochastic and uncertain processes—such as aircraft pushbacks, taxiway movements, runway holdings and take-offs—at an aggregated network level.

Traditional airside modelling encompasses a variety of approaches, including statistical methods [4], stochastic queuing models [3], [5], and microsimulation methods [6], [7]. While statistical methods and queuing network models provide valuable insights, they often fail to capture congestion caused by factors beyond runway queuing, such as delays at network nodes due to conflicts [3]. Furthermore, although microsimulation models, if well calibrated, could accurately describe the network traffic dynamics, they typically require substantial computational resources and time, which limits their effectiveness for real-time applications. In contrast, macroscopic modeling approaches offer a more scalable and computationally efficient alternative by focusing on aggregate traffic flows rather than individual aircraft movements. By capturing the overall dynamics of the airside system, macroscopic models can provide timely insights into congestion patterns and enable rapid decision-making, making them well-suited for real-time applications and large-scale operational planning [8]. Despite their advantages, there is a notable lack of well-developed macroscopic models specifically tailored for airside traffic management.

Inspired from road traffic modelling literature, this paper proposes adapting the Macroscopic Fundamental Diagram (MFD) to model the dynamics of traffic flow and congestion on the airside. First introduced by Godfrey [9] in 1969 and later formalized by Geroliminis and Daganzo [10] in 2008, the MFD provides a representation of traffic dynamics for an urban road network. Irrespective of the specific origins and destinations, the MFD [11] could characterize the overall behavior of network traffic by capturing the relationship between flow Q, density K, and average speed V at an aggregate level across a network [12]. Flow, Q, measured in vehicles (or aircraft) per

hour, represents the rate at which units of traffic pass through a network (or a specific point on the network). In the context of airside operations, flow is analogous to the throughput of the network via the runway. Density, K, measured in vehicles (or aircraft) per kilometer, indicates the concentration of vehicles within a network or along a certain segment of the network. Average speed, V, typically in kilometers per hour (km/h), represents the mean speed at which traffic moves through the network. In other words, flow indicates the efficiency of the system, density reflects the extent of congestion, and average speed shows how fast traffic is moving. Understanding the relationship between these variables helps in diagnosing congestion patterns and predicting system performance under various scenarios.

To the best of our understanding, only two existing works—those by Yang et al. [8] and Wang et al. [13]—have focused on modeling the MFD for airport airside networks, albeit with limitations. Yang et al. [8] were the first to demonstrate the existence of an MFD for an airport airside network, highlighting an aggregate relationship between taxiing-out traffic, arrival landing rates, and runway throughput to inform off-block control or departure metering strategies. However, for Singapore Changi Airport, we found little to no correlation between taxiing-out traffic, arrival landing rates, and runway throughput, suggesting that the relationships observed by Yang et al. may not be universally applicable. Wang et al. [13] claimed to use the MFD to model departing traffic for taxi-out time prediction. However, the aggregate curve they refer to (in Figure 2 of their paper) as the MFD—relating the takeoff rate to the number of departing aircraft on the ground—while valuable, overlooks key flow-density-speed relationships that are the focus of this paper.

In contrast, this study presents a comprehensive method for constructing an airside MFD using 3D aircraft trajectory data (location in latitude/longitude and time stamps), offering new insights into the relationships between airside traffic variables like flow, density, and speed (refer Figure 1). Additionally, it investigates the spatial-temporal factors contributing to congestion, providing a more nuanced understanding of congestion dynamics. The proposed contributions of this study are as follows.

1) This study presents a methodology for constructing an airside MFD using three-dimensional aircraft trajectory data. The approach includes data filtering and pre-processing steps, such as map matching, to derive key airside traffic variables—flow, density, and speed—using A-SMGCS data from Singapore Changi Airport.
2) This study examines the impact of traffic demand (high vs low) and mode of runway operations (segregate vs mix) on airside network flow. This analysis contributes to understanding congestion formation and dissipation in the temporal domain.
3) This study presents a Generalized Macroscopic Fundamental Diagram (GMFD) to quantify the impact of inhomogeneity on airside network flow. A detailed investigation into the relationship between network density and inhomogeneity provides insights into how traffic tends to concentrate on a few taxi routes, especially during periods of congestion.

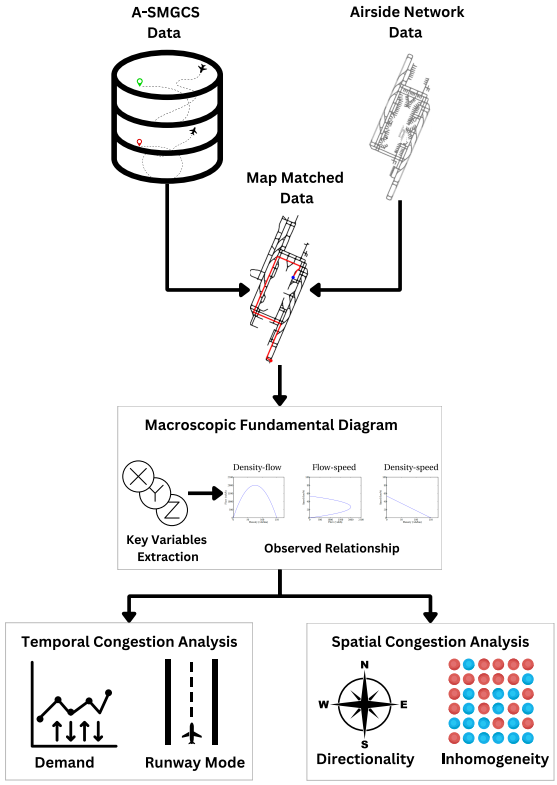

Figure 1. The concept diagram illustrates the methodology for constructing an MFD for an airside network. The MFD, which characterizes the relationships between key macroscopic traffic variables, enables investigation of spatial-temporal factors contributing to congestion. This approach provides insights into airside traffic dynamics, aiding in optimizing the airside network capacity utilization.

II. Data

This section introduces the A-SMGCS data and Changi Airport's airside network, followed by data filtering and pre-processing steps, including map-matching to align aircraft trajectory data with the airside network.

A. Description and Data Filtering

1) A-SMGCS data: In this paper, A-SMGCS data spanning from February 2018 to April 2018, excluding March 30th and 31st, has been utilized, covering a total of 87 days. The dataset provides detailed information related to the surface movement of aircraft in Changi's airside network. Key elements of this dataset include the date of operation, flight call sign, and aircraft type. Additionally, it captures time stamps at one-second intervals, along with corresponding location stamps in latitude and longitude. The dataset also includes the assigned gate or stand for each aircraft, as well as the mean flight level or altitude.

To ensure the accuracy and relevance of the analysis, data filtering was performed. En-route or airborne part of the trajectories, identified by data points above the airport's

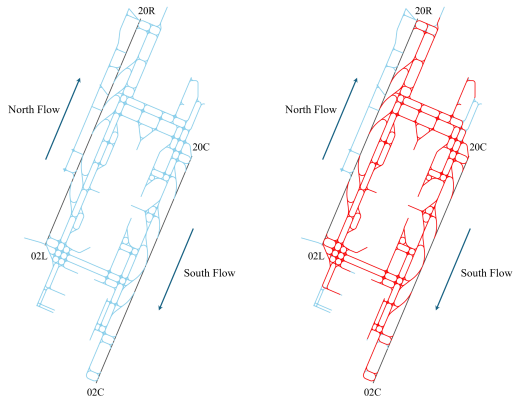

Figure 2. (Left) Singapore Changi Airport airside network, with blue edges representing taxiways and black edges representing runways. Runways 02L and 02C handle north-bound traffic, while runways 20C and 20R handle south-bound traffic. (Right) Red edges indicate the links where aircraft movements have been recorded in the dataset.

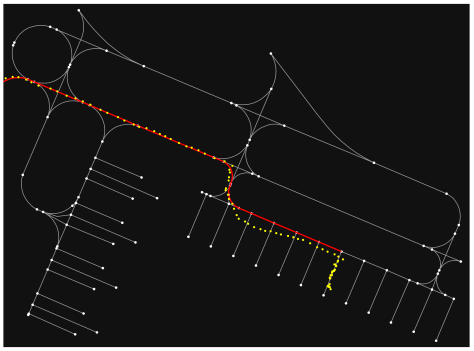

Figure 3. The spatial map-matching illustrates the conversion of yellow trajectory points from a departing flight into a red taxiway path on the airside graph.

elevation level, were excluded to focus solely on ground operations. Ground vehicle trajectories were also removed from the analysis, as their movements, unlike arriving and departing aircraft, lack predefined itineraries in flight plans. Additionally, incomplete aircraft ground trajectories, defined as those with fewer than 10 data points, were excluded in the analysis. The 87-day A-SMGCS dataset included 89,362 trajectory records. After applying data processing and filtering, including the removal of erroneous trajectories identified during the map-matching process, over 96% of the total trajectories (85,883 valid trajectories) were retained for analysis in this study.

2) Changi Airport Airside Network: The airside network is represented as a node-link graph $\mathcal{G}(N, E)$, where the edges E correspond to taxiways and runways, and the nodes N represent their connecting points (as shown in Figure 2 (Left)). In this study, the graph $\mathcal{G}(N, E)$ was generated using python-based OSMNX module [14], based on publicly available OpenStreetMap data. For Singapore Changi Airport, the infrastructure data was extracted using the 'aeroway' tag, while tags such as 'aerodrome,' 'apron,' and 'terminal' were filtered out. The graph is further refined by removing nodes that did not represent intersections or dead-ends. The resulting airside graph consists of 1058 nodes and 1,435 edges, with the average, minimum, and maximum edge lengths being 79.13 meters, 1.25 meters, and 916.97 meters, respectively. In the subsequent analyses, the links with aircraft movement history were identified and filtered. These links, as shown in Figure 2 (Right) in red, represent the network used for extracting the relevant variables (refer section III-A) for further analysis.

B. Data Preprocessing: Map-Matching

The A-SMGCS system tracks aircraft movements, including position and velocity, at one-second intervals. This high-frequency data results in a large volume of information, along with noise [15]. To address this challenge, the tracking data is map-matched with the airport taxiway network using the method described in [15], [16]. The map-matching process is carried out in two key steps: spatial map-matching and temporal map-matching. As shown in Figure 3, spatial map-matching aligns the aircraft's recorded positions with the corresponding taxiway segments in the airside network. This step generates a sequence of taxi segments representing the aircraft's movement, while also filtering out spatial noise in the tracking data. The temporal map-matching step supplants this network-based representation with time and speed information of the aircraft. Each aircraft in a taxi segment is assigned a start and end time, reflecting when the aircraft enters and exits the taxi segment, providing a more comprehensive view of the movement. The method also records timestamps at various points along the taxi segment, along with the corresponding distance the aircraft has traveled. This approach avoids the assumption of a constant speed across the entire taxi segment, allowing for more precise trajectory analysis.

III. Macroscopic Fundamental Diagram for Airport Airside Network

This section outlines the methodology for constructing an MFD for an airport airside network using key traffic variables—flow, density, and speed—derived from three-dimensional aircraft trajectory data, followed by an analysis of congestion dynamics and a detailed examination of the flow-density relationship to illustrate the transition between uncongested and congested traffic states.

A. Macroscopic Traffic Variables: Flow, Density, and Speed

This section discusses the calculation of density, flow, and speed, which are essential for constructing an MFD. The network-level MFD can be expressed using three-dimensional aircraft trajectory data [17], as follows:

$$Q(w) = \frac{d(w)}{L_{xy} \times \Delta t} \tag{1}$$

$$K(w) = \frac{t(w)}{L_{xy} \times \Delta t} \tag{2}$$

$$V(w) = \frac{Q(w)}{K(w)} = \frac{d(w)}{t(w)} \tag{3}$$

where, w is a 3D region encompassing the airport network (in the x-y plane) and time (in the (z)-dimension) during which aircraft taxi. $Q(w)$ and $K(w)$ refer to the average flow and density of w, while $d(w)$ and $t(w)$ are the total distance traveled and the total time spent by aircraft in w, respectively. Moreover, L_{xy} shows the total length of network on x-y plane corresponding to w and Δt is the height of w in time. For the time duration Δt, the analysis in this study has been standardized to 15-minute intervals. The standardization ensures that all variables are derived using the same temporal framework for accurate comparison. The interested reader may refer [18] for more details.

B. Characterization of Congestion using Macroscopic Fundamental Diagram

MFD captures the relationships between flow-density, speed-density, and speed-flow. Figure 4 illustrates all three representations of the MFD, which are similar to the Greenshields fundamental diagrams [19]. In the flow-density plane (refer Figure 4(Top)), flow increases with density up to a critical density beyond which the airside network transitions into the congestion branch, resulting in decreased flow as density rises. The speed-flow plane (refer Figure 4(Middle)) reveals two distinct branches: one representing uncongested conditions characterized by high speeds and high flows, and the other indicating congested conditions with lower speeds and reduced flows. This duality in the speed-flow relationship highlights the complexity of traffic dynamics, emphasizing how different traffic states can coexist under varying conditions. In the speed-density plane (refer Figure 4(Bottom)), high speeds are observed at low densities, with speed gradually decreasing as density increases. The Q and K values are significantly lower (scaled down) in Figure 4 than those observed in road transportation due to the large L_{xy} ($64.3km$) of the Changi airside network (refer equations 1 and 2).

An airside traffic state can be characterized by its density, flow, and speed. According to equation (3), specifying any two of these variables is sufficient to determine the third. Moreover, if a unique relationship between the variables existed, the MFD would allow one variable to determine the entire state. However, the scatter observed in Figure 4 suggests this relationship is not strictly unique.

C. In-Depth Analysis of Flow-Density Relationship

Let us examine two extreme scenarios in the relationship between average network flow and density, as illustrated in Figure 5, which follows the parabolic form of Greenshields' fundamental diagram. In the first scenario, there are no aircraft present on the airside (surface) network. Consequently, with a density of 0, the flow is also 0, as indicated by equation (3). In contrast, in the second scenario, the density in the airside network is so high that the speed drops to 0—an occurrence that

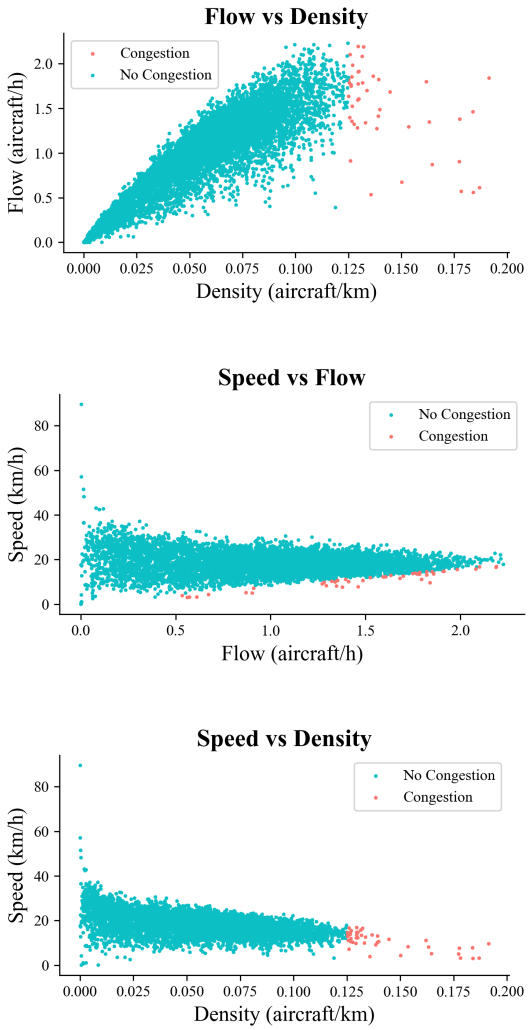

Figure 4. Macroscopic Fundamental Diagram for the airside network in different planes. (Top) Flow vs. density: Flow increases with density up to a critical point, after which a further increase in density leads to congestion and declining flow. (Middle) Speed vs. flow: Two branches—one with high speeds and flows under uncongested conditions, and another with lower speeds and reduced flows during congestion—illustrate the complexity of traffic dynamics and coexistence of different traffic states. (Bottom) Speed vs. density: Higher speeds are observed at low densities, while congestion reduces speeds as density increases.

is theoretically possible but rarely observed in practice—due to gridlock throughout the network. Again, applying equation (3), we find that the flow in this case is also 0. Between these two extremes exist various traffic states where the flow is greater than zero. Assuming a continuous relationship between flow and density, the peak of the curve represents the network flow capacity, while the density corresponding to this capacity is termed the critical density. Both critical density and network capacity are essential traffic control parameters that influence the shape of the MFD. As illustrated in Figure 5, these parameters delineate the boundary between the uncongested and congested branches of the MFD curves, reflecting the optimal

performance of the network. In the uncongested branch, traffic flow increases as density increases. In the congested branch, however, traffic flow decreases as density increases.

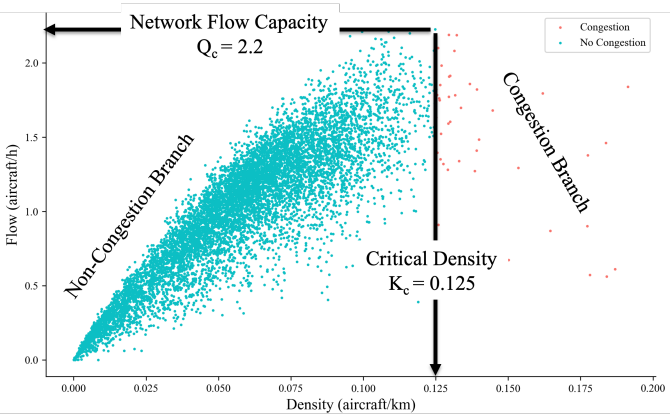

Figure 5. Flow-density relationship for the Singapore Changi Airport airside network. The curve shows two distinct branches: the non-congestion branch, where flow increases with density, upto the network flow capacity, marked at $Q_c = 2.2$ aircraft/h, and the congestion branch, where flow decreases beyond a critical density ($K_c = 0.125$ aircraft/km). In total, 44 data points (15-minute intervals), shown in red, fall within the congested branch, representing 11 hours out of 2077 hours of airside operations. This transition between branches illustrates how increasing density eventually leads to reduced overall flow as congestion builds.

IV. Investigation into the Underlying Factors of Airside Congestion

This section defines the underlying factors contributing to airside congestion, focusing on temporal factors such as traffic demand and runway operation modes, as well as spatial factors including traffic inhomogeneity and flow directionality.

A. Temporal Congestion Factors

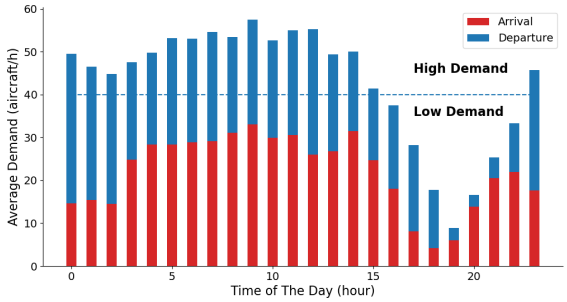

Figure 6. Average traffic demand (arrivals and departures) by time of day, represented in UTC. The blue horizontal dashed line at 40 aircraft movements per hour distinguishes high demand (above 40) from low demand (40 or below) periods.

1) Demand: Figure 6 represents the average hourly demand at Singapore Changi Airport (based on 87 days of A-SMGCS data). It is evident that demand fluctuates throughout the day, with certain hours experiencing greater aircraft movements. Considering that the average hourly demand at Changi Airport is 42 aircraft movements per hour (approximately 10 movements every 15 minutes), we have established a threshold of 40 aircraft movements per hour to differentiate between high and low demand periods. This threshold effectively categorizes demand levels, with values above 40 indicating high demand and those at 40 or below reflecting low demand.

2) Runway Operation Mode: Mix mode runway operations at a two-runway airport like Singapore Changi Airport refer to using a single runway for both arrivals and departures, while the other runway may also be active but in various operational modes (e.g., dedicated for arrivals, departures, or mix as well). This setup optimizes runway capacity by dynamically adjusting operations to meet varying demand for arrivals and departures, improving efficiency during peak periods or traffic surges [20]. To identify (15-minute) periods of mix-mode runway operations using aircraft trajectory data, we set a threshold of more than one arrival and one departure movement on the same runway (could be either runway).

B. Spatial Congestion Factors

1) Inhomogeneity: Homogeneous traffic conditions imply that aircraft are evenly spread throughout the network, while inhomogeneous conditions occur when traffic concentrates around specific bottlenecks, such as near runways or key taxiways. We use the standard deviation of density as measure of inhomogeneity, denoted as $\gamma(w)$ [21]:

$$\gamma(w) = \sqrt{\frac{\sum_i (k_i(w) - K(w))^2}{N}} \tag{4}$$

$$k_i(w) = \frac{t_i(w)}{L_i \times \Delta t} \tag{5}$$

where, $k_i(w)$ denotes the density of each link i in w, $t_i(w)$ denotes the total time which aircraft spent traveling on the link i in w, N denotes the total count of links in the network and L_i is the physical length of link i.

2) Directionality: Flow directions at Singapore Changi Airport can be categorized into North and South flows (refer Figure 2). These flow directions are primarily influenced by wind direction and magnitude, with North flows being the most common at Changi. To assess the impact of flow direction on average network flows, we assign a flow direction to each 15-minute interval. If 50% or more of the aircraft take off or land in the southbound direction during an interval, it is classified as having a South flow; otherwise, it is categorized as having a North flow.

V. Analytical Methods for Congestion Investigation

This section outlines the methodologies used to analyze airside congestion, employing time-space diagrams to visualize congestion patterns under varying traffic demands, the Mann-Whitney U test to assess statistical significance in flow-density distributions across different operational modes and flow directions, and the GMFD to investigate the impact of inhomogeneity on traffic flow.

A. Temporal Congestion Analysis: Time-Space Diagrams

Time-space diagram analysis is employed to investigate congestion patterns at Changi Airport across different traffic demand levels. This well-established method visualizes aircraft movement over time and distance, making it particularly useful for understanding how congestion forms and evolves under varying conditions. The analysis involves plotting the trajectory of each aircraft in both time and space, which allows for the identification of patterns such as flow continuity, bottlenecks, and queuing. By examining traffic during both low and high demand periods, distinct congestion behaviors can be observed.

B. Statistical Test of Significance: Mann-Whitney U test

The Mann-Whitney U test will be employed to examine the differences in flow-density distributions across different operational modes (mix mode vs segregate mode) and different flow directions (North vs South flow). The Mann-Whitney U test is a non-parametric method used to compare the distributions of two independent samples. Unlike the t-test, it does not assume normality or equal variances, making it a robust choice for various data distributions. The test ranks all observations from both samples, calculates the U statistic based on these ranks, and tests the null hypothesis that the samples come from the same distribution. A significant U value indicates a difference between the samples.

C. Spatial Congestion Analysis: Generalized Macroscopic Fundamental Diagram (GMFD) and Inhomogeneity

We aim to study the extent to which inhomogeneity contributes to a reduction in average flow. The GMFD [21] is employed to investigate the impact of inhomogeneity on traffic flow within Changi Airport's airside network. The GMFD extends the traditional MFD by incorporating inhomogeneity, which refers to the uneven distribution of traffic across the network.

In addition to assessing the impact of inhomogeneity, we quantify the relationship between network density and inhomogeneity. This analysis will illustrate the relevance of the potential problem of nucleation, where one part of the network becomes congested and attracts further congestion, while other parts remain in free-flow conditions [22].

VI. Results

This section presents results, including an analysis of the impact of traffic demand on congestion, statistical comparisons between different runway operations and directionality, and an investigation into the role of inhomogeneity in airside network flow.

A. Temporal Congestion: Traffic Demand

MFD shape is significantly influenced by the level of traffic demand (number of arrivals and departures) as illustrated in Figure 7. During high demand, the MFD is displaced farther from the origin compared to the MFD for low demand, indicating higher initial flow and density values. This displacement

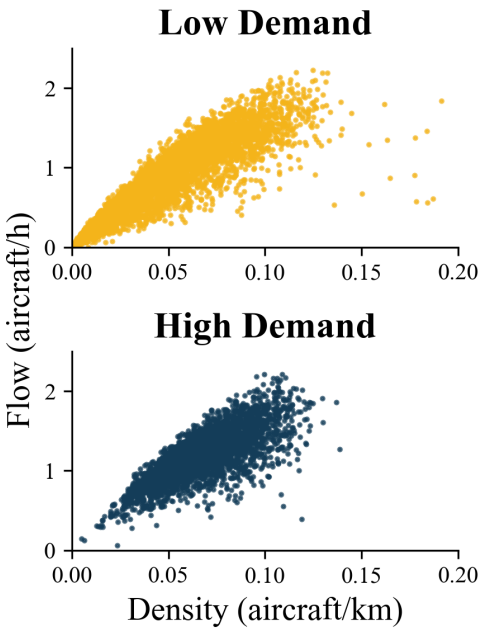

Figure 7. Effect of traffic demand on the shape of MFD. The MFD for high demand periods starts farther from the origin than that for low demand. Surprisingly, the low demand MFD exhibits a more distinct congestion branch.

suggests that when traffic demand is higher, there is a relatively higher initial buildup of flow and density as more aircraft occupy the airside network. In contrast, the MFD corresponding to low demand is closer to the origin, implying a lower initial flow due to fewer aircraft movements. Interestingly, even with reduced traffic levels, the low demand MFD exhibits a more pronounced congestion branch. This suggests that the airside network can still experience congestion with fewer aircraft, warranting further analysis.

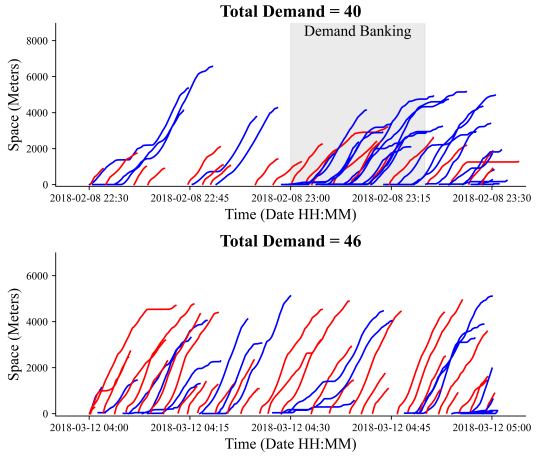

Figure 8. Time-space plots for low and high demand periods reveal that low demand (Top) can still lead to congestion due to banked operations, while evenly spaced high demand (Bottom) allows for higher flows without overwhelming the airside network (see Figure 7).

A deeper analysis of the different demand periods (low

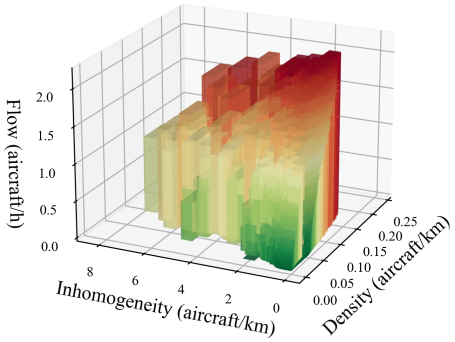

Figure 9. The effect of average density and inhomogeneity on average flow is depicted, with a color gradient ranging from low (green) to high (red) flows. This gradient demonstrates that density is a crucial factor in determining network flow. However, for a given network density, an increase in inhomogeneity further reduces the flow, as evidenced by the lower flow values associated with higher inhomogeneity levels.

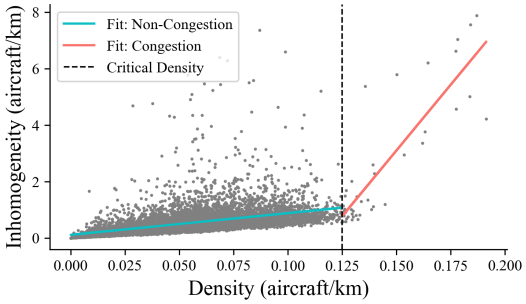

Figure 10. Relationship between average density and inhomogeneity: Inhomogeneity increases with average density. In the non-congestion phase, this increase is gradual. The steeper slope in the congestion phase suggests that at higher average densities, the network becomes inhomogeneous more quickly, as traffic load tends to concentrate on a few similar taxi routes.

and high), using the time-space diagrams (see Figure 8), provides additional insights into traffic dynamics. During low demand periods, there is evidence of demand banking, where traffic is temporally stacked. This is common in hub airports, where fluctuating demand can lead to large queues throughout the day [15], [20], [23]. This could explain the pronounced congestion observed in the low demand MFD, where periods of low density are accompanied by short bursts of high density aircraft movements. In contrast, during high demand periods, the time-space diagram reveals a more continuous flow of aircraft, although congestion still accumulates as the network becomes saturated. These figures illustrate that both low and high traffic demand can lead to congestion, but the underlying mechanisms differ: low demand can experience sharp bursts of congestion that dissipate during periods of low activity, while high demand results in a more gradual buildup.

B. Statistical Analysis Results: Mann-Whitney U Test Results

We conducted a statistical analysis of average flow distributions using the Mann-Whitney U test for both mixed and segregate runway operations, as well as for North and South directional flows. At a 95% confidence level ($\alpha = 0.05$), the analysis reveals that mix-mode operations exhibit significantly higher flow values compared to segregate runway operations. However, when comparing flow distributions between the North and South directions, no significant difference was found, implying that directional flows have similar performance under current operational conditions.

C. Spatial Congestion: Relationship Between Inhomogeneity, Density and Flow

The GMFD (refer Figure 9) shows the effect of inhomogeneity in the traffic on the average flow in the network. The inhomogeneity has an influence on the average flow: for the same average density, an increase in inhomogeneity reduces the average flow. While average density is the primary influencing factor, the standard deviation of density also significantly contributes to determining flow throughout the airside network.

The relationship between inhomogeneity and average density is nearly linear, as shown in Figure 10. In both the non-congestion and congestion phases, inhomogeneity increases with average density. In the non-congestion phase, this increase is gradual. The steeper slope in the congestion phase suggests that at higher average densities, the network becomes inhomogeneous more quickly, as traffic load tends to concentrate on a few similar taxi routes. This observation underscores the critical need for ATCOs to more evenly assign taxi routes across the airside, especially during periods of congestion, ultimately leading to improved average flows and network capacity utilization.

VII. Discussion

This study investigates the spatial and temporal factors contributing to congestion and offers insights into how congestion patterns develop and evolve under varying operational conditions. In the temporal domain, it was observed that even during low-demand periods, departure and arrival banks contributed to congestion. To address this common challenge at hub airports, congestion pricing can be employed to effectively distribute arrival and departure banks, resulting in a more balanced flight schedule throughout the day. Additionally, MFDs can be leveraged to implement effective departure metering policies to alleviate congestion. In the spatial domain, a detailed analysis highlighted the issue of nucleation, where congestion in one part of the Changi airside network attracts further congestion, while other areas remain in free-flow conditions [22]. This finding underscores the importance of assigning taxi routes more evenly across the airside, particularly during congested periods, to enhance overall flow and maximize network capacity utilization.

The findings of this study provide valuable insights into airside network operations at Singapore Changi Airport, but the extent to which these results are generalizable to other airports warrants further discussion. The MFD and GMFD approaches effectively capture flow-density relationships and the impact

TABLE I. RESULTS FROM MANN-WHITNEY U TEST FOR AVERAGE FLOW DISTRIBUTIONS.

S.No.	Type	U Statistic	P-value	Conclusion
1	Mode: Segregate Vs Mix	6152929	0.004	Flow is significantly greater in mix mode at $\alpha = 0.05$
2	Directionality: North Vs South	770441	0.492	Not significantly different at $\alpha = 0.05$

of traffic inhomogeneity, but their specific characteristics are influenced by factors such as airport layout, taxiway design, and traffic patterns. Therefore, while the core principles of MFD may apply broadly, the critical density values, flow capacity, and congestion patterns observed at Changi may differ in airports with varying infrastructure and operational modes.

VIII. CONCLUSION

This study has validated the existence and applicability of the MFD for analyzing airside network operations at Singapore Changi Airport using A-SMGCS data. Our analysis reveals a strong relationship between average flow, density, and speed, providing valuable insights into airside traffic dynamics. We examined the impact of operational factors such as traffic demand levels and runway modes. Our findings suggest that congestion can occur even during low demand periods if the demand is temporally concentrated or banked. Moreover, mix-mode runway operations result in significantly higher flow compared to segregate modes. However, flow differences between North and South directions were not significant. Furthermore, the GMFD highlighted the importance of traffic inhomogeneity. An uneven distribution of traffic reduces overall flow, particularly during congestion. These results emphasize the potential to improve airside capacity utilization and mitigate congestion by evenly distributing airside traffic across both temporal and spatial domains, i.e., minimizing schedule banks and ensuring a balanced allocation of taxi routes. This study's key limitation is the exclusion of weather conditions from the MFD analysis, despite their significant impact on airside operations; future research should integrate weather data.

ACKNOWLEDGMENT

This research is supported by the National Research Foundation, Singapore, and the Civil Aviation Authority of Singapore, under the Aviation Transformation Programme. Any opinions, findings and conclusions or recommendations expressed in this material are those of the author(s) and do not reflect the views of National Research Foundation, Singapore and the Civil Aviation Authority of Singapore.

REFERENCES

[1] H. Ali, D.-T. Pham, S. Alam, and M. Schultz, "A deep reinforcement learning approach for airport departure metering under spatial–temporal airside interactions," *IEEE Transactions on Intelligent Transportation Systems*, vol. 23, no. 12, pp. 23 933–23 950, 2022.

[2] A. R. Odoni, J. Bowman, D. Delahaye, J. J. Deyst, E. Feron, R. J. Hansman, K. Khan, J. K. Kuchar, N. Pujet, and R. W. Simpson, "Existing and required modeling capabilities for evaluating atm systems and concepts," Tech. Rep., 2015.

[3] I. Simaiakis, "Modeling and control of airport departure processes for emissions reduction," Ph.D. dissertation, Massachusetts Institute of Technology, 2009.

[4] H. Ali, R. Delair, D.-T. Pham, S. Alam, and M. Schultz, "Dynamic hot spot prediction by learning spatial-temporal utilization of taxiway intersections," in *2020 International Conference on Artificial Intelligence and Data Analytics for Air Transportation*. IEEE, 2020.

[5] N. Pujet, B. Delcaire, and E. Feron, "Input-output modeling and control of the departure process of congested airports," in *Guidance, Navigation, and Control Conference and Exhibit*, 1999, p. 4299.

[6] G. J. Couluris, R. K. Fong, M. B. Downs, N. Mittler, D. Signor, A. Stassart, and T. Hsiao, "A new modeling capability for airport surface traffic analysis," in *2008 IEEE/AIAA 27th Digital Avionics Systems Conference*. IEEE, 2008, pp. 3–E.

[7] R. Mori, "Aircraft ground-taxiing model for congested airport using cellular automata," *IEEE Transactions on Intelligent Transportation Systems*, vol. 14, no. 1, pp. 180–188, 2012.

[8] L. Yang, S. Yin, K. Han, J. Haddad, and M. Hu, "Fundamental diagrams of airport surface traffic: Models and applications," *Transportation Research Part B: Methodological*, vol. 106, pp. 29–51, Dec. 2017.

[9] J. Godfrey, "The mechanism of a road network," *Traffic Engineering & Control*, vol. 8, no. 8, 1969.

[10] N. Geroliminis and C. F. Daganzo, "Existence of urban-scale macroscopic fundamental diagrams: Some experimental findings," *Transportation Research Part B: Methodological*, vol. 42, no. 9, pp. 759–770, 2008.

[11] C. F. Daganzo, "Urban gridlock: Macroscopic modeling and mitigation approaches," *Transportation Research Part B: Methodological*, vol. 41, no. 1, pp. 49–62, 2007.

[12] C. F. Daganzo and M. J. Cassidy, "Effects of high occupancy vehicle lanes on freeway congestion," *Transportation research part B: methodological*, vol. 42, no. 10, pp. 861–872, 2008.

[13] S. Wang, L. Yang, Y. Wang, and W. Cong, "A data and model-driven approach to predict congestion of departure traffic at airport," in *2022 Integrated Communication, Navigation and Surveillance Conference (ICNS)*. IEEE, 2022, pp. 1–15.

[14] G. Boeing, "Osmnx: New methods for acquiring, constructing, analyzing, and visualizing complex street networks," *Computers, Environment and Urban Systems*, vol. 65, pp. 126–139, 2017.

[15] H. Ali, "Data driven and learning based approaches for integrated landside airside operations optimization," 2022.

[16] T.-N. Tran, D.-T. Pham, and S. Alam, "A map-matching algorithm for ground movement trajectory representation using a-smgcs data," in *2020 International Conference on Artificial Intelligence and Data Analytics for Air Transportation (AIDA-AT)*. IEEE, 2020, pp. 1–8.

[17] M. Saberi, H. S. Mahmassani, T. Hou, and A. Zockaie, "Estimating network fundamental diagram using three-dimensional vehicle trajectories: extending edie's definitions of traffic flow variables to networks," *Transportation Research Record*, vol. 2422, no. 1, pp. 12–20, 2014.

[18] M. Johari, M. Keyvan-Ekbatani, L. Leclercq, D. Ngoduy, and H. S. Mahmassani, "Macroscopic network-level traffic models: Bridging fifty years of development toward the next era," *Transportation Research Part C: Emerging Technologies*, vol. 131, p. 103334, 2021.

[19] B. D. Greenshields, J. R. Bibbins, W. Channing, and H. H. Miller, "A study of traffic capacity," in *Highway research board proceedings*, vol. 14, no. 1. Washington, DC, 1935, pp. 448–477.

[20] H. Ali, D.-T. Pham, and S. Alam, "Toward greener and sustainable airside operations: A deep reinforcement learning approach to pushback rate control for mixed-mode runways," *IEEE Transactions on Intelligent Transportation Systems*, 2024.

[21] V. L. Knoop, H. Van Lint, and S. P. Hoogendoorn, "Traffic dynamics: Its impact on the macroscopic fundamental diagram," *Physica A: Statistical Mechanics and its Applications*, vol. 438, pp. 236–250, 2015.

[22] V. L. Knoop, P. B. van Erp, L. Leclercq, and S. P. Hoogendoorn, "Empirical mfds using google traffic data," in *2018 21st International Conference on Intelligent Transportation Systems (ITSC)*. IEEE, 2018, pp. 3832–3839.

[23] H. Ali, D.-T. Pham, S. Alam, and M. Schultz, "Integrated airside landside framework to assess passenger missed connections with airport departure metering," in *International Conference on Research in Air Transportation*, 2022.